J|A|C|S
ARTICLES
Published on Web 09/11/2004

Substituent-Dependent Photoinduced Intramolecular Charge Transfer in *N*-Aryl-Substituted *trans*-4-Aminostilbenes

Jye-Shane Yang,* Kang-Ling Liau, Chin-Min Wang, and Chung-Yu Hwang

Contribution from the Department of Chemistry and Center for Nano Science and Technology, National Central University/UST, Chung-Li, Taiwan 32054

Received April 26, 2004; E-mail: jsyang@cc.ncu.edu.tw

Abstract: The photochemical behavior of *trans*-4-(*N*-arylamino)stilbene (**1**, aryl = 4-substituted phenyl) in solvents more polar than THF is strongly dependent on the substituent in the *N*-aryl group. This is attributed to the formation of a twisted intramolecular charge transfer (TICT) state for those with a methoxy (**1OM**), methoxycarbonyl (**1CO**), or cyano (**1CN**) substituent but not for those with a methyl (**1Me**), hydrogen (**1H**), chloro (**1Cl**), or trifluoromethyl (**1CF**) substituent. On the basis of the ring-bridged model compounds **3**−**6**, the TICT states for **1CN** and **1CO** result from the twisting of the anilino-benzonitrilo C−N bond, but for **1OM** it is from the twisting of the stilbenyl-anilino C−N bond, both of which are distinct from the TICT states previously proposed for *N*,*N*-dimethylaminostilbenes.

Introduction

The electronic excited states of arylamines possess more or less the character of intramolecular charge transfer (ICT) from the amino nitrogen to the arene, and those having the ICT configuration as the main component are often referred to as ICT states. While many ICT-based arylamines have been investigated as nonlinear optical materials,[1] two-photon-absorbing chromophores,[2] electrooptical switches,[3] chemical sensors,[4] and fluorescence probes,[5] characterization of their ICT states (e.g., electronic nature and molecular geometry) is far from straightforward, even for a simple molecule such as 4-(*N*,*N*-dimethylamino)benzonitrile (DMABN). Since the first observation by Lippert et al.,[6] the phenomenon of dual fluorescence for DMABN has led to numerous theoretical and experimental studies to account for the origin of the ICT fluorescence.[6−13] Several distinct models have been proposed, including a twisting of the dimethylamino (donor, D)−benzonitrilo (acceptor, A) single bond that results in a nearly perpendicular D−A geometry (twisted intramolecular charge transfer, TICT),[7−10] an in-plane bending of the cyano group (rehybridization by intramolecular charge transfer, RICT),[11] and a pyramidalization (wagged

(1) (a) Marder, S. R.; Perry, J. W. *Science* **1994**, *263*, 1706−1707. (b) Verbiest, T.; Burland, D. M.; Jurich, M. C.; Lee, V. Y.; Miller, R. D.; Volksen, W. *Science* **1995**, *268*, 1604−1606. (c) Whitaker, C. M.; Patterson, E. V.; Kott, K. L.; McMahon, R. J. *J. Am. Chem. Soc.* **1996**, *118*, 9966−9973. (d) Nandi, P. K.; Mandal, K.; Kar, T. *Chem. Phys. Lett.* **2003**, *381*, 230−238.
(2) (a) Albota, M.; Beljonne, D.; Brédas, J. L.; Ehrlich, J. E.; Fu, J.-Y.; Heikal, A. A.; Hess, S. E.; Kogej, T.; Levin, M. D.; Marder, S. R.; McCord-Maughon, D.; Perry, J. W.; Röckel, H.; Rumi, M.; Subramaniam, G.; Webb, W. W.; Wu, X.-L.; Xu, C. *Science* **1998**, *281*, 1653−1656. (b) Kogej, T.; Beljonne, D.; Meyers, F.; Perry, J. W.; Marder, S. R.; Brédas, J. L. *Chem. Phys. Lett.* **1998**, *298*, 1−6. (c) Reinhardt, B. A.; Brott, L. L.; Clarson, S. J.; Dillard, A. G.; Bhatt, J. C.; Kannan, R.; Yuan, L.; He, G. S.; Prasad, P. N. *Chem. Mater.* **1998**, *10*, 1863−1874. (d) Lee, W.-H.; Lee, H.; Kim, J.-A.; Choi, J.-H.; Cho, M.; Jeon, S.-J.; Cho, B. R. *J. Am. Chem. Soc.* **2001**, *123*, 10658−10667. (e) Wang, X.; Zhou, Y.; Zhou, G.; Jiang, W.; Jiang, M. *Bull. Chem. Soc. Jpn.* **2002**, *75*, 1847−1854.
(3) La Clair, J. J. *Angew. Chem., Int. Ed.* **1999**, *38*, 3045−3047.
(4) (a) Morozumi, T.; Anada, T.; Nakamura, H. *J. Phys. Chem. B* **2001**, *105*, 2923−2931. (b) Xiao, Y.; Qian, X. *Tetrahedron Lett.* **2003**, *44*, 2087−2091. (c) Yang, J.-S.; Hwang, C.-Y.; Hsieh, C.-C.; Chiou, S.-Y. *J. Org. Chem.* **2004**, *69*, 719−726. (d) Yang, J.-S.; Lin, Y.-D.; Lin, Y.-H.; Liao, F.-L. *J. Org. Chem.* **2004**, *69*, 3517−3525.
(5) La Clair, J. J. *Angew. Chem., Int. Ed.* **1998**, *37*, 325−329.
(6) (a) Lippert, E.; Lüder, W.; Moll, F.; Nägele, W.; Boos, H.; Prigge, H.; Seibold-Blankenstein, I. *Angew. Chem.* **1961**, *73*, 695−706. (b) Lippert, E.; Lüder, W.; Boos, H. In *Advances in Molecular Spectroscopy*; Mangini, A., Ed.; Pergamon Press: Oxford, 1962; pp 443−457.
(7) (a) Rotkiewicz, K.; Grellmann, K. H.; Grabowski, Z. R. *Chem. Phys. Lett.* **1973**, *19*, 315−318. (b) Grabowski, Z. R.; Rotkiewicz, K.; Siemiarczuk, A.; Cowley, D. J. Baumann, W. *Nouv. J. Chim.* **1979**, *3*, 443−454. (c) Rettig, W. *Angew. Chem., Int. Ed. Engl.* **1986**, *25*, 971−988. (d) Rettig, W.; Maus, M. In *Conformational Analysis of Molecules in Excited States*; Waluk, J., Ed.; Wiley-VCH: New York, 2000; Chapter 1, pp 1−55. (e) Grabowski, Z. R.; Rotkiewicz, K. *Chem. Rev.* **2003**, *103*, 3899−4031.
(8) (a) Rettig, W.; Bliss, B.; Dirnberger, K. *Chem. Phys. Lett.* **1999**, *305*, 8−14. (b) Rettig, W.; Zietz, B. *Chem. Phys. Lett.* **2000**, *317*, 187−196. (c) Rettig, W.; Lutze, S. *Chem. Phys. Lett.* **2001**, *341*, 263−271. (d) Dobkowski, J.; Wójcik, J.; Kozminski, W.; Kolos, R.; Waluk, J.; Michl, J. *J. Am. Chem. Soc.* **2002**, *124*, 2406−2407. (e) Rotkiewicz, K.; Rettig, W.; Detzer, N.; Rothe, A. *Phys. Chem. Chem. Phys.* **2003**, *5*, 998−1002. (f) Dobkowski, J.; Michl, J.; Waluk, J. *Phys. Chem. Chem. Phys.* **2003**, *5*, 1027−1031. (g) Kwok, W. M.; Ma, C.; George, M. W.; Grills, D. C.; Matousek, P.; Parker, A. W.; Phillips, D.; Toner, W. T.; Towrie, M. *Phys. Chem. Chem. Phys.* **2003**, *5*, 1043−1050. (h) Saigusa, H.; Iwase, E.; Nishimura, M. *J. Phys. Chem. A* **2003**, *107*, 3759−3763.
(9) (a) Mennucci, B.; Toniolo A.; Tomasi, J. *J. Am. Chem. Soc.* **2000**, *122*, 10621−10630. (b) Parusel, A. B. J.; Rettig, W.; Sudholt, W. *J. Phys. Chem. A* **2002**, *106*, 804−815. (c) Jödicke, C. J.; Lüthi, H. P. *J. Am. Chem. Soc.* **2003**, *125*, 252−264. (d) Jödicke, C. J.; Lüthi, H. P. *J. Chem. Phys.* **2003**, *119*, 12852−12865. (e) Rappoport, D.; Furche, F. *J. Am. Chem. Soc.* **2004**, *126*, 1277−1284.
(10) (a) Serrano-Andrés, L.; Merchán, M.; Roos, B. O.; Lindh, R. *J. Am. Chem. Soc.* **1995**, *117*, 3189−3204. (b) Jödicke, C. J.; Lüthi, H. P. *J. Chem. Phys.* **2002**, *117*, 4146−4156. (c) Jödicke, C. J.; Lüthi, H. P. *J. Chem. Phys.* **2002**, *117*, 4157−4167.
(11) (a) Sobolewski, A. L.; Domcke, W. *Chem. Phys. Lett.* **1996**, *250*, 428−436. (b) Sobolewski, A. L.; Domcke, W. *Chem. Phys. Lett.* **1996**, *259*, 119−127.
(12) Schuddeboom, W.; Jonker, S. A.; Warman, J. M.; Leinhos, U.; Kühnle, W.; Zachariasse, K. A. *J. Phys. Chem.* **1992**, *96*, 10809−10819.
(13) (a) von der Haar, T.; Hebecker A.; Il'ichev, Y.; Jiang, Y.-B.; Kühnle, W.; Zachariasse, K. A. *Recl. Trav. Chim. Pays-Bas* **1995**, *114*, 430−442. (b) Zachariasse, K. A.; Grobys, M.; von der Haar, T.; Hebecker A.; Il'ichev, Y. V.; Jiang, Y.-B.; Morawski, O.; Kühnle, W. *J. Photochem. Photobiol. A: Chem.* **1996**, *102*, 59−70. (c) Zachariasse, K. A.; Grobys, M.; von der Haar, T.; Hebecker A.; Il'ichev, Y. V.; Morawski, O.; Rückert, I.; Kühnle, W. *J. Photochem. Photobiol. A: Chem.* **1997**, *105*, 373−383. (d) Il'ichev, Y. V.; Kühnle, W.; Zachariasse, K. A. *J. Phys. Chem. A* **1998**, *102*, 5670−5680. (e) Zachariasse, K. A. *Chem. Phys. Lett.* **2000**, *320*, 8−13. (f) Demeter, A.; Zachariasse, K. A. *Chem. Phys. Lett.* **2003**, *380*, 699−703. (g) Zachariasse, K. A.; Druzhinin, S. I.; Bosch, W.; Machinek, R. *J. Am. Chem. Soc.* **2004**, *126*, 1705−1715.

intramolecular charge transfer, WICT)[12] or a planarization (planar intramolecular charge transfer, PICT) of the amino group.[13] Among them, the TICT model has gained widespread acceptance and appears to be the conclusion of the numerous debates over the past decades.[7−13]

Despite the well-documented photochemistry and photophysics of *trans*-stilbene and its derivatives,[14] the nature of the ICT state of aminostilbenes is still under active discussion.[15−24] When compared with DMABN, the participation of the double-bond torsion (trans−cis isomerization) in the excited-state manifold and the lack of steady-state dual fluorescence for aminostilbenes in both nonpolar and polar solvents often complicate the data analysis. On the basis of theoretical predictions and experimental comparisons with ring-bridged model compounds,[15−19] an emissive TICT state resulting from the twisting of the anilino-styrenyl C−C single bond has been proposed for *N*,*N*-dimethylaminostilbene (DS) and its cyano- and nitro-substituted derivatives in polar solvents. However, controversies were soon raised regarding the nature of the emissive state as a planar or a twisted configuration and the necessity of a TICT state in interpreting the photochemical properties of aminostilbenes.[20−24] For example, a spectral evolution of transient fluorescence could be attributed to a relaxation of the solvent cage instead of the conformational relaxation of the excited molecule.[22] In addition, a pronounced ring-bridging effect on the fluorescence quantum yield could result from a particular substituent effect on the reaction hypersurface from the planar (^{1}t*) to the double-bond twisted (^{1}p*) states (the two-state model) rather than the participation of an additional TICT state (the three-state model).[21] Evidently, further studies are required to reach a satisfactory conclusion on these issues for aminostilbenes.

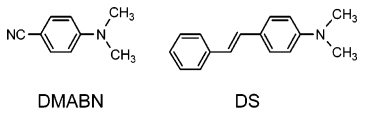

DMABN DS

We report herein the results of our systematic studies on the excited-state properties of *N*-aryl-substituted *trans*-4-aminostilbenes (**1**) and the related model compounds **2**−**6**, which have provided a unique opportunity for gaining insights into the ICT states of aminostilbenes. When compared with the *N*,*N*-dialkyl derivatives (e.g., DS), the *N*-aryl-substituted 4-aminostilbenes have inherently greater fluorescence quantum yields and longer fluorescence lifetimes due to the prominent "amino conjugation effect".[25,26] Thus, a breakdown of such an *N*-aryl conjugation effect by twisting either a C−N or a C−C single bond should result in a state with distinct fluorescence properties. Provided that structural relaxations of **1** toward a TICT state are present and become more efficient in more polar solvents, as proposed for the case of DS,[15] a dramatic change of the ICT fluorescence of **1** on going from nonpolar to polar solvents should be observed. Another advantage offered by *N*-aryl vs *N*-alkyl systems is that the donor strength could be tuned to a large extent by changing the *N*-aryl substituents, without significantly changing the size of molecules. It has been shown that the donor strength plays an important role in observing the TICT fluorescence for DMABN and its analogues.[10] More importantly, our results turn out to have a direct linkage to the TICT paradigm of DMABN.[7−10] The seven *N*-aryl derivatives in **1** could be divided into three distinct categories in terms of their solvent-dependent fluorescence properties. While the one consisting of **1CN** and **1CO** displays a DMABN-like TICT fluorescence, the other two categories (**1OM** vs **1Me**, **1H**, **1Cl**, and **1CF**) lack dual fluorescence but offer an analogy with and a difference from the first one in other excited-state properties, respectively. In conjunction with the *N*-methyl (**2**) and the ring-bridged model compounds (**3**−**6**), the substituent-dependent ICT states for **1** will be elucidated and discussed.

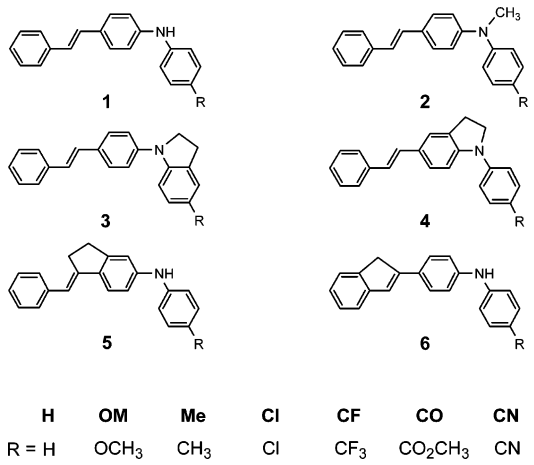

Results

Synthesis and Molecular Structure. The synthesis of aminostilbenes **1** is straightforward, based on palladium-catalyzed amination reactions[27] between *trans*-4-bromostilbene and the corresponding commercially available 4-substituted

(14) (a) Saltiel, J.; Charlton, J. L. In *Rearrangements in Ground and Excited States*; de Mayo, P., Ed.; Academic Press: New York, 1980; Vol. 3, pp 25−89. (b) Saltiel, J.; Sun, Y.-P. In *Photochromism, Molecules and Systems*; Dürr, H., Bouas-Laurent, H., Eds.; Elsevier: Amsterdam, 1990; pp 64−164. (c) Waldeck, D. H. *Chem. Rev.* **1991**, *91*, 415−436. (d) Görner, H.; Kuhn, H. J. *Adv. Photochem.* **1995**, *19*, 1−117.
(15) Létard, J.-F.; Lapouyade, R.; Rettig W. *J. Am. Chem. Soc.* **1993**, *115*, 2441−2447.
(16) (a) Rettig, W.; Majenz, W. *Chem. Phys. Lett.* **1989**, *154*, 335−341. (b) Lapouyade, R.; Czeschka, K.; Majenz, W.; Rettig, W.; Gilabert, E.; Rullière, C. *J. Phys. Chem.* **1992**, *96*, 9643−9650. (c) Abraham, E.; Oberlé, J.; Jonusauskas, G.; Lapouyade, R.; Rullière, C. *J. Photochem. Photobiol. A: Chem.* **1997**, *105*, 101−107. (d) Papper, V.; Pines, D.; Likhtenshtein, G.; Pines, E. *J. Photochem. Photobiol. A: Chem.* **1997**, *111*, 87−96. (e) Abraham, E.; Oberlé, J.; Jonusauskas, G.; Lapouyade, R.; Rullière, C. *Chem. Phys.* **1997**, *214*, 409−423. (f) Pines, D.; Pines, E.; Rettig, W. *J. Phys. Chem. A* **2003**, *107*, 236−242.
(17) (a) Amatatsu, Y. *Theor. Chem. Acc.* **2000**, *103*, 445−450. (b) Amatatsu, Y. *Chem. Phys.* **2001**, *274*, 87−98.
(18) (a) Gruen, H.; Görner, H. *J. Phys. Chem.* **1989**, *93*, 7144−7152. (b) Lapouyade, R.; Kuhn, A.; Létard, J.-F.; Rettig, W. *Chem. Phys. Lett.* **1993**, *208*, 48−58.
(19) Létard, J.-F.; Lapouyade, R.; Rettig, W. *Chem. Phys. Lett.* **1994**, *222*, 209−216.
(20) Seydack, M.; Bendig, J. *J. Phys. Chem. A* **2001**, *105*, 5731−5733.
(21) (a) Il'ichev, Y. V.; Kühnle, W.; Zachariasse, K. A. *Chem. Phys.* **1996**, *211*, 441−453. (b) Kovalenko, S. A.; Schanz, R.; Senyushkina, T. A.; Ernsting, N. P. *Phys. Chem. Chem. Phys.* **2002**, *4*, 703−707.
(22) Eilers-König, N.; Kühne, T.; Schwarzer, D.; Vöhringer, P.; Schroeder, J. *Chem. Phys. Lett.* **1996**, *253*, 69−76.
(23) Rechthaler, K.; Köhler, G. *Chem. Phys. Lett.* **1996**, *250*, 152−158.
(24) (a) Lewis, F. D.; Kalgutkar, R. S.; Yang, J.-S. *J. Am. Chem. Soc.* **1999**, *121*, 12045−12053. (b) Lewis, F. D.; Weigel, W. *J. Phys. Chem. A* **2000**, *104*, 8146−8153. (c) Lewis, F. D.; Weigel, W.; Zuo, X. *J. Phys. Chem. A* **2001**, *105*, 4691−4696.
(25) Yang, J.-S.; Chiou, S.-Y.; Liau, K.-L. *J. Am. Chem. Soc.* **2002**, *124*, 2518−2527.
(26) Yang, J.-S.; Wang, C.-M.; Hwang, C.-Y.; Liau, K.-L.; Chiou, S.-Y. *Photochem. Photobiol. Sci.* **2003**, *2*, 1225−1231.
(27) (a) Wolfe, J. P.; Wagaw, S.; Marcoux, J.-F.; Buchwald, S. L. *Acc. Chem. Res.* **1998**, *31*, 805−818. (b) Hartwig, J. F. *Angew. Chem., Int. Ed.* **1998**, *37*, 2046−2067.

Scheme 1

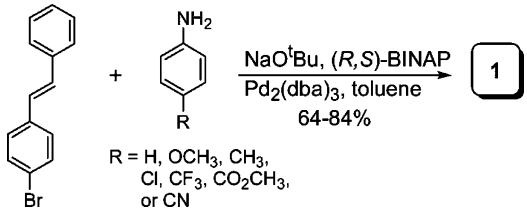

Scheme 2

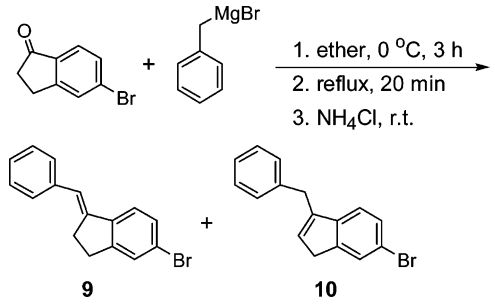

anilines (Scheme 1). Typical procedures have been previously reported for the synthesis of **1H**.[25]

Model compounds **2**−**6** possessing a methoxy (e.g., **2OM**) or a cyano (e.g., **2CN**) substituent also have been prepared. Compounds **2** were prepared by *N*-methylation[28] of the corresponding compounds **1**. Except for the cases of **4**, the synthetic methodology for the bridged derivatives is similar to that for **1**, namely, via a Pd-catalyzed coupling of bromostilbenes and anilines with the desired bridged structures in either substrates. The 5-methoxyindoline (**7**) for the synthesis of **3OM** was prepared from the reduction of 5-methoxyindole by sodium cyanoborohydride.[29] The corresponding precursor for compound **3CN** is 5-bromoindoline (**8**), and the amination reaction was followed by a cyanization reaction[30] that converts the bromo group to a cyano group. The bromostilbene **9** for the formation of **5OM** and **5CN** could, in principle, be prepared by a nucleophilic addition of benzylmagnesium bromide to 5-bromo-1-indanone, followed by acid-catalyzed dehydration (Scheme 2), a method analogous to the synthesis of 1-benzalindane.[31] However, the separation of **9** from its isomer **10** is not feasible. Whereas a pure sample of the final product **5OM** is not yet available,[32] compound **5CN** could be readily purified by column chromatography. The synthesis of compound **6H** has recently been reported,[26] and the same intermediate **11** was employed for the formation of **6OM** and **6CN**.

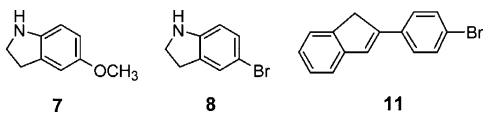

As shown in Scheme 3, the syntheses of **4OM** and **4CN** started with the *N*-arylation of indoline, followed by a formylation[33] at the 5-position of indoline. A conventional Horner−Wadsworth−Emmons reaction[34] then led to the desired aminostilbenes **4**.

(28) Borch, R. F.; Hassid, A. I. *J. Org. Chem.* **1972**, *37*, 1673−1674.
(29) Gangjee, A.; Vasudevan, A.; Queener, S. F. *J. Med. Chem.* **1997**, *40*, 479−485.
(30) Ikan, R.; Rapaport, E. *Tetrahedron* **1967**, *23*, 3823−3827.
(31) Plentl, A. A.; Bogert, M. T. *J. Am. Chem. Soc.* **1941**, *63*, 989−995.

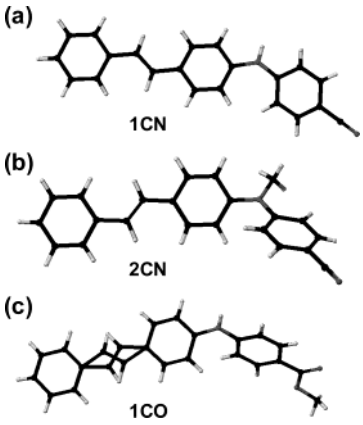

Figure 1. X-ray crystal structures of (a) **1CN**, (b) **2CN**, and (c) **1CO** (double bond disordered).

Scheme 3

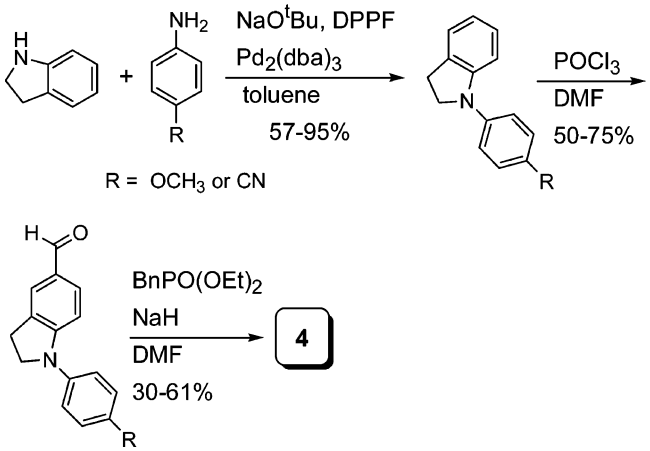

The X-ray crystal structures of **1CO**, **1CN**, and **2CN** have been determined (Figure 1). The stilbene moiety is essentially planar in all three cases. Whereas the *N*-phenyl and the terminal styrenyl groups in **2CN** are located on the same side (the syn conformation) with respect to the long molecular axis, they are on the opposite side (the anti conformation) in **1CN**, and there is a syn−anti disorder in the case of **1CO**. These observations are in accord with our previous conformational analysis for aminostilbenes **1H**, **2H**, and **6H**, where the syn and the anti conformers were calculated to be of similar energies, with a difference less than 0.3 kcal/mol.[25,26] Our previous results also suggested a shallow minimum for their ground-state potential energy surfaces, and in solutions there should exist a large distribution of conformers with varied ring−ring torsional and amino wagging angles.[26] This is more likely a common feature for all aminostilbenes **1**−**6**.

Electronic Spectra. All the aminostilbenes **1**−**6** in hexane and acetonitrile display a single intense long-wavelength absorption band. The corresponding absorption maxima (λ_{abs}) are reported in Table 1, and typical spectra are presented in Figure 2 for **1OM** and **1CN**. For comparison, the data of DS are also included. In general, an electron-donating (ED) or electron-withdrawing (EW) substituent at the para position of the *N*-phenyl group shifts the absorption maximum to the red (e.g., **1OM** vs **1H**) and to the blue (e.g., **1CN** vs **1H**), respectively. In addition, the spectra in acetonitrile are bathochromic, hypochromic, and broadened when compared with those in hexane. However, the solvatochromic shift is rather small, which

Table 1. Maxima of UV Absorption (λ_{abs}) and Fluorescence (λ_f), Fluorescence Band Half-Width ($\Delta\nu_{1/2}$), 0,0 Transition ($\lambda_{0,0}$), and Stokes Shifts ($\Delta\nu_{st}$) of Aminostilbenes **1**−**6** and DS in Hexane (Hex) and Acetonitrile (MeCN)[a]

compd	solvent	λ_{abs} (nm)	λ_f (nm)[b]	$\Delta\nu_{1/2}$ (cm^{-1})	$\lambda_{0,0}$ (nm)[c]	$\Delta\nu_{st}$ (cm^{-1})[d]
1H	Hex	346	381 (399)	2956	370	2655
	MeCN	351	442	3547	393	5785
1Me	Hex	349	385 (402)	2808	374	2679
	MeCN	354	457	3866	398	6367
1Cl	Hex	344	382 (399)	2913	369	2892
	MeCN	351	437	3582	390	5607
1CF	Hex	340	376 (395)	2775	366	2816
	MeCN	347	421	3428	383	5065
1OM	Hex	349	389 (409)	2782	378	2946
	MeCN	356	502	6218	398	8170
1CO	Hex	348	384 (403)	2526	373	2694
	MeCN	358	425 [530]	8687	388	4292
1CN	Hex	341	381 (399)	2712	370	3079
	MeCN	352	425 [517]	8086	387	4880
2OM	Hex	350	406 (425)	2946	386	3941
	MeCN	356	577	9658[g]	382	10759
2CN	Hex	335	397 (412)	2851	379	4662
	MeCN	342	[539][e]	5052	397	10859
3OM	Hex	374	440	3856	403	4011
	MeCN[f]	378				
3CN	Hex	357	391 (412)	2147	383	2436
	MeCN	369	438	3564	400	4269
4OM	Hex	367	408 (430)	2362	398	2738
	MeCN	373	483	3429	423	6106
4CN	Hex	366	407 (420)	2759	393	2752
	MeCN	379	[567][e]	5931[g]	408	8749
5CN	Hex	345	392 (406)	3141	376	3475
	MeCN	359	[535][e]	6019[g]	392	9164
6OM	Hex	345	385 (405)	3117	375	3669
	MeCN	351	472	6312	389	7304
6CN	Hex	347	391 (405)	3129	375	3243
	MeCN	354	[530][e]	5804[g]	388	9381
DS[h]	Hex	347	379	3425		2433
	MeCN	351	440	3306		5763

[a] Fluorescence data are from corrected spectra. [b] The second vibronic band is given in parentheses, and the long-wavelength emission band is given in brackets. [c] The value of $\lambda_{0,0}$ was obtained from the intersection of normalized absorption and fluorescence spectra. [d] $\Delta\nu_{st} = \nu_{abs} - \nu_f$. [e] The short-wavelength emission could not be resolved. [f] Fluorescence too weak to be reliably determined. [g] Values are estimated due to the incomplete spectra. [h] Data from ref 15.

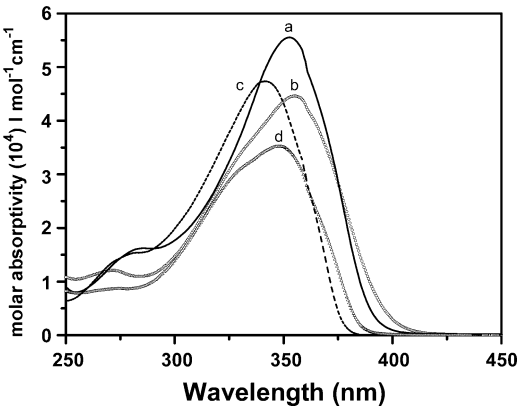

Figure 2. UV−vis absorption spectra of **1OM** (curves a and b) and **1CN** (curves c and d) in hexane (curves a and c) and acetonitrile (curves b and d).

indicates a small difference between the dipole moments of the Franck−Condon (FC) excited state and the ground state. According to our previous studies on **1H**, **2H**, and **6H**, the long-wavelength band can be attributed to electronic transitions delocalized throughout the whole molecule with a charge-transfer character of mainly the HOMO (amino nitrogen) → LUMO (stilbene) transition.[25,26] On the basis of the results of semiempirical INDO/S-SCF-CI (ZINDO) calculations[35] for the AM1-optimized[36] structures of **1OM** and **1CN**, the introduction of substituents at the *N*-phenyl group has only a small effect on the contribution of the HOMO → LUMO configuration to the description of the lowest excited singlet state (S_1) (i.e., ∼85−86% for **1OM** and **1CN** as compared with ∼89% for **1H**).

The fluorescence spectra of all aminostilbenes **1**−**6** are structured in hexane but become less structured in toluene and completely structureless in more polar solvents. In addition, unlike the absorption spectra, the fluorescence spectra shift significantly to the red with increasing solvent polarity, indicating a strong ICT character for the fluorescent states (^{1}t*) of these aminostilbenes. The fluorescence maxima (λ_f), the half-bandwidth ($\Delta\nu_{1/2}$), the 0,0 transitions ($\lambda_{0,0}$), and the Stokes shift ($\Delta\nu_{st}$) of **1**−**6** in hexane and acetonitrile are reported in Table 1.

For the compound series **1**, the size of the solvatochromic shifts and the shape of the fluorescence spectra in polar solvents strongly depend on the substituent. As shown in Figure 3, the structureless fluorescence spectra are in a normal Gaussian shape for **1H**, **1Me**, **1Cl**, and **1CF**, but they are significantly broadened for **1OM** and become dual fluorescent for **1CO** and **1CN** in solvents more polar than THF. It should be noted that an emission longer than 650 nm would be less accurate due to the limitation of our instrument. When the short emission bands for **1CO** and **1CN** were taken into account, the magnitude of the shift on going from hexane to acetonitrile is in the order **1OM** > **1Me** > **1H** > **1Cl** > **1CF** > **1CN** ∼ **1CO**, which is roughly parallel with the relative electron-donating ability of the substituents. It is interesting to note that the energies of the fluorescence maxima of **1** correlate better with the Hammett σ^+ than with the σ constants (Figure 4).[37] In hexane, a nice linear relationship could be observed for **1**, except for **1CO** and **1CN**. The lower-than-predicted fluorescence peak energies for the latter two species could be attributed to the conjugation effect of the π-substituents. While the linear correlation among **1Me**, **1H**, **1Cl**, and **1CF** is retained in dichloromethane and acetonitrile, the data points for **1OM** become off the line, which is more severe in acetonitrile than in dichloromethane. It should also be noted that both the fluorescence excitation and emission spectra of **1** in hexane and acetonitrile are essentially independent of the emission and excitation wavelengths, respectively, and the former closely follow the absorption spectra.[38] Evidently, the conformers in **1** should have similar electronic properties, as previously observed for **1H**,[25] and the dual emitters in **1CN** and **1CO** should result from the same FC state.

The dipole moment (μ_e) of the fluorescent state can be estimated from the slope (m_f) of the plot of the energies of the

(32) Compound **5OM** is weakly fluorescent and very sensitive to the room light, and more than one photoproduct has been detected by HPLC.
(33) Jutz, C. *Adv. Org. Chem.* **1976**, *9*, 225−342.
(34) Wadsworth, W. S., Jr. *Org. React.* **1977**, *25*, 73−253.
(35) Zerner, M. C.; Leow, G. H.; Kirchner, R. F.; Mueller-Westerhoff, U. T. *J. Am. Chem. Soc.* **1980**, *102*, 589−599.
(36) Dewar, M. J. S.; Zoebisch, E. G.; Healy, E. F.; Stewart, J. J. P. *J. Am. Chem. Soc.* **1985**, *107*, 3902−3909.
(37) Lowry, T. H.; Richardson, K. S. *Mechanism and Theory in Organic Chemistry*; Harper & Row: New York, 1987; p 144.
(38) See Supporting Information for details.

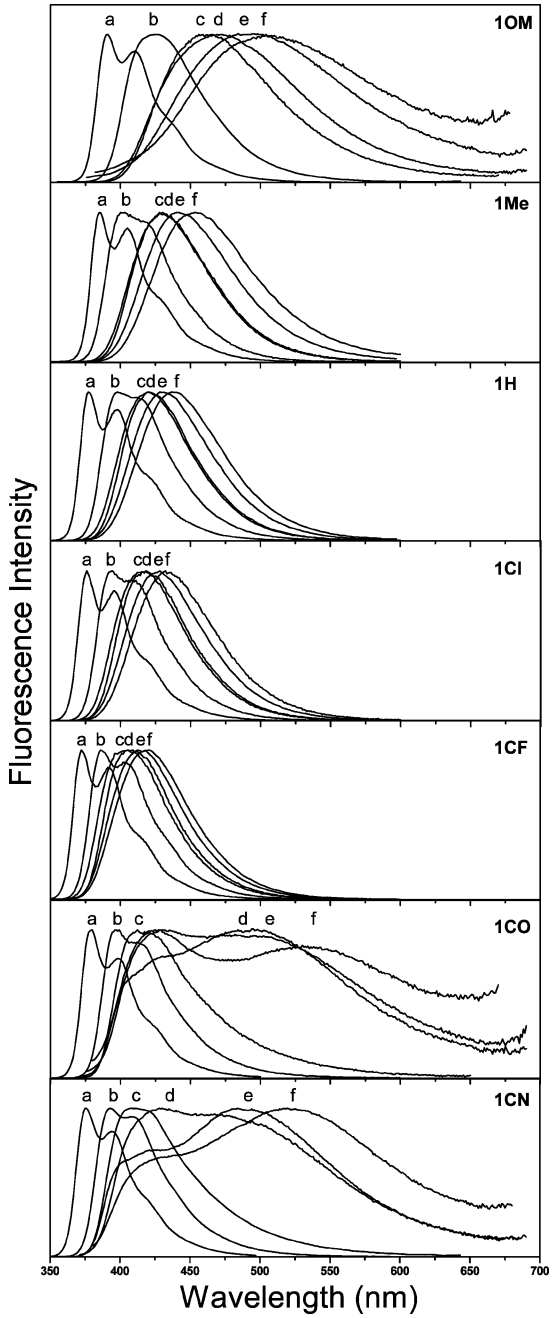

Figure 3. Normalized fluorescence spectra of aminostilbenes **1** in (a) hexane, (b) toluene, (c) THF, (d) dichloromethane, (e) acetone, and (f) acetonitrile.

fluorescence maxima against the solvent parameter Δf according to eq 1:[15,38,39]

$$\nu_f = -[(1/4\pi\epsilon_0)(2/hca^3)]\,[\mu_e(\mu_e - \mu_g)]\,\Delta f + \text{constant} \quad (1)$$

where

$$\Delta f = (\epsilon - 1)/(2\epsilon + 1) - 0.5(n^2 - 1)/(2n^2 + 1) \quad (2)$$

and

$$a = (3M/4N\pi d)^{1/3} \quad (3)$$

where ν_f is the fluorescence maximum, μ_g is the ground-state dipole moment, a is the solvent cavity (Onsager) radius, which could be derived from the Avogadro number (N), molecular weight (M), and density (d), and ϵ, ϵ_0, and n are the solvent dielectric, vacuum permittivity, and the solvent refractive index, respectively. The value of μ_g was calculated using the MOPAC-AM1 algorithm. The calculated ground-state dipole moment is **1CF** > **1CN** > **1CO** > **1Cl** > **1OM** > **1Me** > **1H**, and the dipole moment is essentially oriented toward the *N*-stilbenyl and the *N*-aryl group for the ED- and the EW-substituted species, respectively. Assuming that the angle between the ground- and the excited-state dipoles of the EW-substituted derivatives is ca. 120°, the calculated ground-state dipole would have a component vector of $0.5\mu_g$ (i.e., $\cos(120°)\mu_g$) in a direction opposite to that of the N → stilbene excited-state dipole. Accordingly, a negative value of $-0.5\mu_g$ was adopted for eq 1 in calculating the μ_e for **1Cl** and **1CF** and the short-wavelength bands of **1CO** and **1CN**. In contrast, the long-wavelength emitting states of **1CO** and **1CN** are more likely to have a dipole in the same direction as that for the ground-state dipoles (vide infra). These results, along with the corresponding data for DS, are summarized in Table 2.

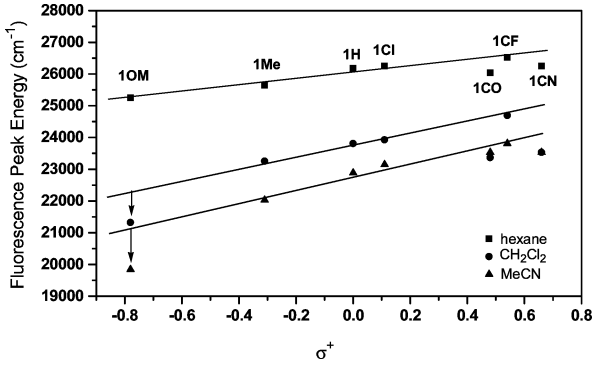

Figure 4. Correlation diagram of the energies of the fluorescence maxima against the Hammett σ^+ constants for **1** in hexane, dichloromethane, and acetonitrile. The short-wavelength emission maxima are adopted for **1CN** and **1CO**.

Table 2. Ground- and Excited-State Dipole Moments for **1**, **3CN**, **4OM**, and DS

compd	a (Å)[a]	m_f (cm^{-1})[b]	μ_g (D)[c]	μ_e (D)
1OM	4.93	14351	0.98	13.6
1Me	4.84	11493	0.94	11.8
1H	4.76	9973	0.84	10.8
1Cl	4.66	9851	1.70	9.5[d]
1CF	4.96	8346	4.37	9.0[d]
1CO[e]	5.07	7880 (17132)	2.88	9.4[d] (16.4)
1CN[e]	4.90	8672 (17106)	4.25	9.1[d] (16.4)
3CN	5.04	7329	4.21	8.7[d]
4OM	5.06	10467	0.18	11.7
DS[f]	4.53	12335	2.41	11.8

[a] Onsager radius calculated by eq 3 with $d = 1.0$ for **1OM**, **1Me**, **1H**, **1CO**, **1CN**, **3CN**, and **4OM**, 1.1 for **1CF**, and 1.2 g/cm^3 for **1Cl**. [b] Calculated on the basis of eq 1. [c] Calculated by AM1. [d] Calculated with $-0.5\mu_g$. [e] The values for the long-wavelength emission state are given in parentheses. [f] Data from ref 15.

The dependence of the fluorescence spectra of **1OM** and **1CN** in hexane and acetonitrile on temperature has been investigated (Figure 5). In hexane, the fluorescence intensity of **1OM** is significantly reduced upon heating from −40 to 50 °C, but it is insensitive to the change in temperature for **1CN**. The results

(39) (a) Liptay, W. Z. *Z. Naturforsch.* **1965**, *20a*, 1441. (b) Lippert, E. *Z. Elecktrochem.* **1957**, *61*, 962−975. (c) Mataga, N.; Kaifu, Y.; Koizumi, M. *Bull. Chem. Soc. Jpn.* **1956**, *29*, 465−470.

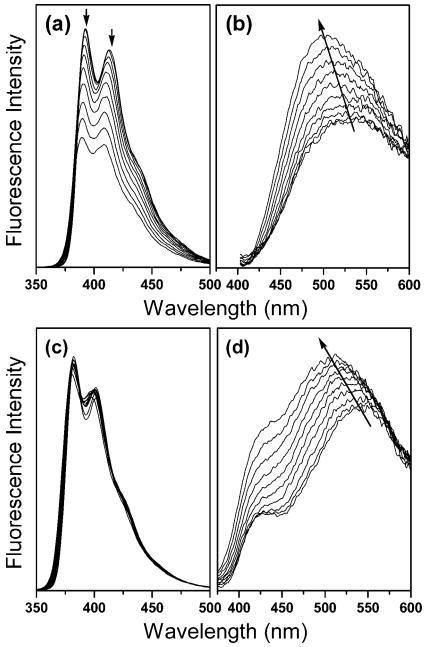

Figure 5. Temperature dependence of the fluorescence spectra of **1OM** in (a) hexane and (b) acetonitrile and of **1CN** in (c) hexane and (d) acetonitrile recorded at intervals of 10 °C between −40 and 50 °C. The arrows indicate the direction of fluorescence response upon raising the temperature.

are different in acetonitrile, where the fluorescence is enhanced and blue-shifted for both **1OM** and **1CN** upon raising the temperature. Previous studies on **1H** have shown that its fluorescence intensity undergoes a monotonic decrease with increasing temperature in both hexane and acetonitrile.[25] Evidently, the excited-state behavior of aminostilbenes **1** is significantly affected by the *N*-aryl substituent.

When compared with **1OM** and **1CN**, the additional *N*-methyl or methylene bridging group in **2**−**6** affects the electronic spectra more or less, depending on the nature of the *N*-aryl group and the position of the methylene group (Table 1). For instance, the introduction of an *N*-methyl group shifts the absorption maxima of **1CN** to the blue (i.e., **2CN**), but it has only a small effect on that of **1OM** (i.e., **2OM**). In addition, the ring-bridged species have longer wavelength λ_{abs} and λ_f than the corresponding nonbridged compounds **1** and **2**, but compound **6OM** is an exception. The most intriguing observation is probably the narrower fluorescence shape for **3CN** and **4OM** in comparison to the other analogues in polar solvents (Figure 6). In other words, the broad and largely Stokes-shifted fluorescence spectra for **1OM** and **1CN** are also observed for **2OM**−**6OM** and **2CN**−**6CN** in dichloromethane (Figure 7) and acetonitrile, but the solvatofluorochromic shifts and the excited-state dipole moments for **3CN** and **4OM** are more like those for **1CF** and **1Me** (Table 2), respectively.

Quantum Yields and Lifetimes. The fluorescence quantum yields (Φ_f) for aminostilbenes **1**−**6** in a variety of solvents have been determined, and some of these data are reported in Table 3. For the compound series **1**, all derivatives are strongly fluorescent in hexane and toluene, but the values of Φ_f decrease in more polar solvents. The plots of Φ_f against the microscopic solvent polarity parameter, $E_T(30)$,[40] are shown in Figure 8. Whereas the group consisting of **1H**, **1Me**, **1Cl**, and **1CF**

(40) Marcus, Y. *Chem. Soc. Rev.* **1993**, 409−416.

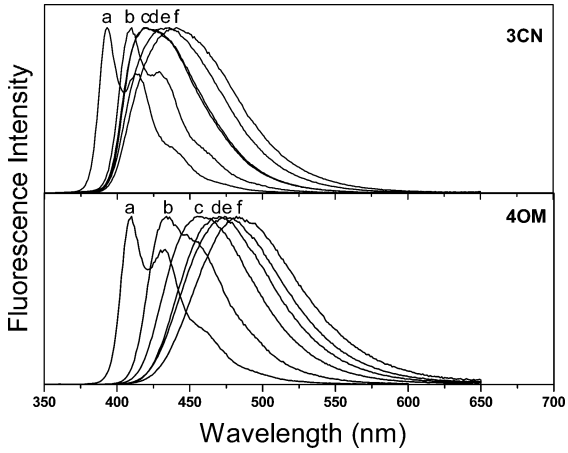

Figure 6. Normalized fluorescence spectra of aminostilbenes **3CN** and **4OM** in (a) hexane, (b) toluene, (c) THF, (d) dichloromethane, (e) acetone, and (f) acetonitrile.

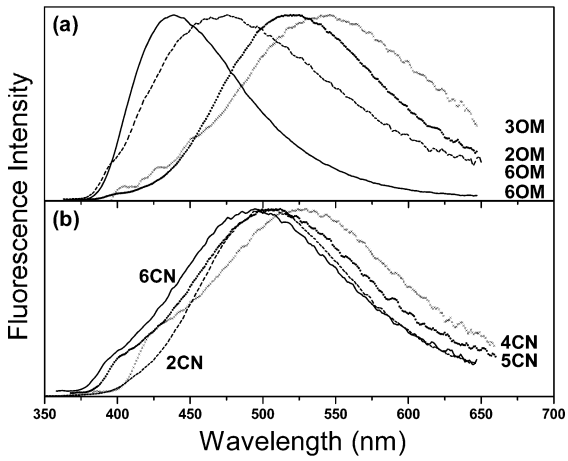

Figure 7. Normalized fluorescence spectra of (a) **2OM**, **3OM**, and **6OM** and (b) **2CN** and **4CN**−**6CN** in dichloromethane. For comparison, the spectra of **6OM** in acetonitrile (the segmented curve in (a)) are included.

follows an essentially linear correlation (Figure 8a), it is a sigmodial curve for the group of **1OM**, **1CO**, and **1CN** (Figure 8b). It is interesting to note that all the substituted derivatives, regardless of ED or EW substituents at the *N*-phenyl group, have a larger value of Φ_f than does **1H** in nonpolar solvents.

Quantum yields for trans → cis photoisomerization (Φ_{tc}) for the compound series **1** in THF and dichloromethane are reported in Table 3. Assuming that the decay of the double bond twisted perpendicular excited state (p*) yields a 1:1 ratio of trans and cis isomers,[14] the sum of the fluorescence and double bond torsion quantum yields ($\Phi_f + 2\Phi_{tc}$) for **1H**, **1Me**, **1Cl**, and **1CF** in both solvents is within the experimental error of 1.0, but it is relatively lower than 1.0 for **1OM**, **1CO**, and **1CN** in THF and even lower in dichloromethane. Evidently, fluorescence and photoisomerization could account for the excited decay of the former cases, but other channels of nonradiative decay should be taken into account for the latter three compounds in polar solvents.

The fluorescence lifetimes (τ_f) of the aminostilbenes **1** in different solvents are provided in Table 3. All decays can be well fit by single-exponential functions, although more than one conformer is expected for **1** in solutions, and there is dual fluorescence for **1CN** and **1CO** in polar solvents. Nonetheless, as demonstrated in dichloromethane, the values of τ_f for **1CO**

Table 3. Quantum Yields for Fluorescence (Φ_f) and Photoisomerization (Φ_{tc}), Fluorescence Decay Times (τ_f), Rate Constants for Fluorescence Decay (k_f), and Nonradiative Decay (k_{nr}) for **1**−**6** and DS in Solutions

compd	solvent	Φ_f	Φ_{tc}	τ_f (ns)[a]	k_f (10^8 s^{-1})	k_{nr} (10^8 s^{-1})
1H	Hex	0.51	0.24[b]	0.89	5.7	5.5
	THF	0.42	0.24	0.87	4.8	6.7
	CH_2Cl_2	0.38	0.34	0.70	5.4	8.9
	MeCN	0.34		0.96	3.5	6.9
1Me	Hex	0.53		0.96	5.1	4.9
	THF	0.55	0.28	1.31	4.2	3.4
	CH_2Cl_2	0.49	0.28	1.15	4.3	4.4
	MeCN	0.41		1.75	2.3	3.4
1Cl	Hex	0.58		1.00	5.8	4.2
	THF	0.53	0.27	0.96	5.5	4.9
	CH_2Cl_2	0.48	0.29	0.75	6.4	6.9
	MeCN	0.43		0.96	4.5	5.9
1CF	Hex	0.68		1.07	6.4	3.0
	THF	0.49	0.18	0.84	5.8	6.1
	CH_2Cl_2	0.43	0.22	0.67	6.4	8.5
	MeCN	0.25		0.67	3.7	11.2
1OM	Hex	0.60	0.10[b]	1.20	5.0	3.3
	THF	0.36	0.05	2.44	1.5	2.6
	CH_2Cl_2	0.24	0.09	2.40	1.0	3.2
	MeCN	0.007		0.32	0.22	31.0
1CO	Hex	0.72		1.22	5.9	2.3
	THF	0.38	0.11	2.19	1.7	2.8
	CH_2Cl_2	0.03	0.04	0.94[d]	0.32	10.3
	MeCN	0.004		0.41	0.10	24.3
1CN	Hex	0.75	0.16[c]	1.30	5.8	1.9
	THF	0.46	0.16	2.70	1.7	2.0
	CH_2Cl_2	0.11	0.14	2.90[d]	0.38	3.1
	MeCN	0.015		0.84	0.18	11.7
2OM	Hex	0.65		2.54	2.6	1.4
	MeCN	0.005		0.56	0.18	17.7
2CN	Hex	0.68		2.52	2.6	1.4
	MeCN	0.02		0.98	0.20	10.0
3OM	Hex	0.81		3.00	2.7	0.63
	MeCN	<0.001				
3CN	Hex	0.81		1.43	5.7	1.3
	CH_2Cl_2	0.81	0.02	1.45	5.6	1.3
	MeCN	0.81		1.71	4.7	1.1
4OM	Hex	0.75		1.54	4.0	2.5
	CH_2Cl_2	0.66	0.25	1.91	3.5	1.8
	MeCN	0.68		2.36	2.4	1.8
4CN	Hex	0.78		1.56	5.0	1.4
	MeCN	0.014		0.38	0.37	25.9
5CN	Hex	0.056		0.12	4.7	78.7
	MeCN	0.005		<0.10	>0.5	>99.5
6OM	Hex	0.84		1.20	6.3	8.3
	MeCN	0.031		0.87	0.36	11.1
6CN	Hex	0.87		1.50	5.8	0.87
	MeCN	0.007		0.11	0.64	90.3
DS[e]	Hex	0.030		0.1[f]	3.0	97
	MeCN	0.037		0.1[f]	3.7	96

[a] The value of τ_f was determined with excitation and emission around the spectral maxima, unless otherwise noted. [b] Containing 10% of THF by reason of solubility. [c] Containing 12% of THF by reason of solubility. [d] An averaged value is adopted. [e] Data from ref 15. [f] Data determined in diethyl ether and ethanol are both 0.1 ns.

(0.63−1.11 ns) and **1CN** (2.31−3.50 ns) are dependent on the emission wavelength and are larger at longer wavelength emissions, a phenomenon not observed for the other derivatives of **1**. In addition, the fluorescence rate constants ($k_f = \Phi_f \tau_f^{-1}$) are comparable for all seven compounds of **1** in hexane, but they are more than 1 order of magnitude smaller for **1OM**, **1CO**, and **1CN** than the others in acetonitrile. The overall nonradiative deactivation ($k_{nr} = 1/\tau_f - k_f$) was also calculated (Table 3). The absence of specific correlation between the log k_{nr} and the emission energy (figure not shown) indicates that internal conversion is unimportant in accounting for the decay of **1H**, **1Me**, **1Cl**, and **1CF**.

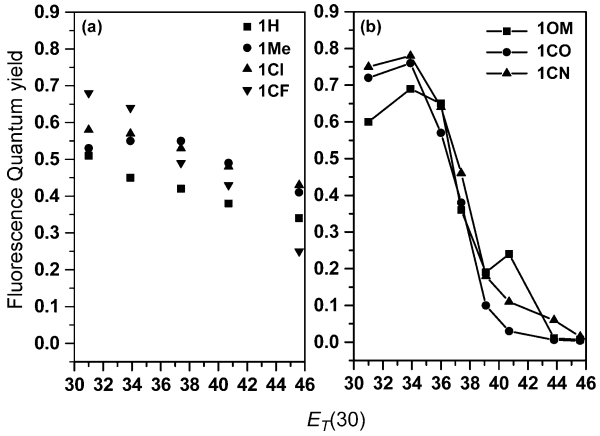

Figure 8. Plots of the fluorescence quantum yield (Φ_f) against the solvent parameter $E_T(30)$ for the compound series **1**. The solvents [$E_T(30)$] are (from left to right) hexane [31.0], toluene [33.9], THF [37.4], dichloromethane [40.7], and acetonitrile [45.6] for both plots (a) and (b), and three more solvents, 1,4-dioxane [36.0], chloroform [39.1], and DMF [43.8], are added for plot (b).

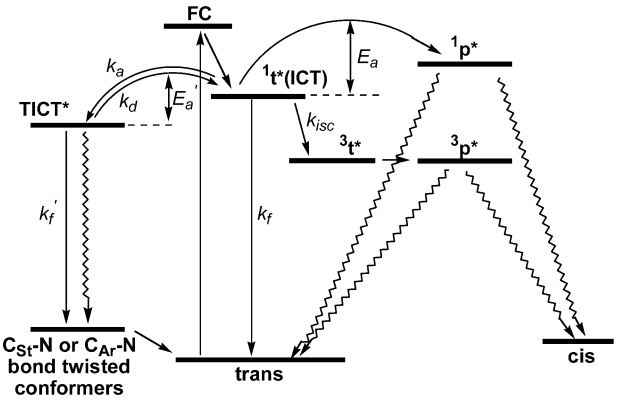

Figure 9. Simplified scheme for the formation and decay of the fluorescent ICT state of *trans*-4-(*N*-arylamino)stilbenes **1**. The C_{St}−N and C_{Ar}−N bonds denote the stilbenyl-anilino and the aryl-anilino C−N bonds, respectively.

The values of Φ_f, τ_f, k_f, and k_{nr} for **2**−**6** in hexane and acetonitrile are also reported in Table 3. In accord with the observations based on fluorescence spectra, the large values of Φ_f and k_f in acetonitrile for **3CN** and **4OM** differentiate them from the other cyano- and methoxy-substituted derivatives. For comparison, the values of Φ_{tc} for **3CN** and **4OM** in dichloromethane were also determined. It should be noted that the restriction of the C=C double bond torsion does not prevent **6CN** and **6OM** from having a low Φ_f value in acetonitrile. In addition, the fluorescence quantum yield is low for **5CN** even in hexane. Nonetheless, the solvent effect on its Φ_f is still significant.

Discussion

A generalized scheme for the photochemical behavior of aminostilbenes **1** is shown in Figure 9. The substituents play an important role in determining the relative energy levels of the excited states and thus the resulting decay pathways. The seven derivatives could be divided into three different groups (I−III), based on their excited-state behavior, which are discussed in the following.

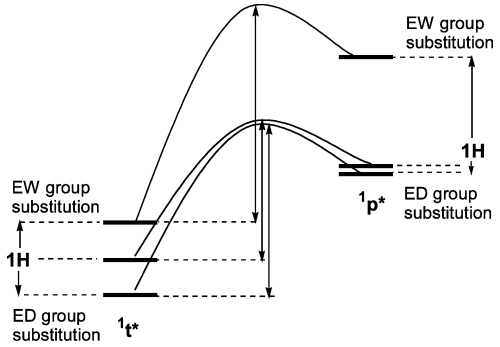

Figure 10. Qualitative representation of the substituent effect on the barrier of $^1t^* \rightarrow {}^1p^*$ double bond torsion in the singlet excited state.

Excited-State Behavior of 1H, 1Me, 1Cl, and 1CF (Group I). The photochemical behavior of **1H** has recently been reported.[25,26] Like the parent *trans*-4-aminostilbene,[24] the decay of excited **1H** is mainly via fluorescence and the double bond torsion reaction (i.e., $\Phi_f + 2\Phi_{tc} \approx 1.0$). However, **1H** displays much higher fluorescence quantum yields and lower trans → cis isomerization quantum yields as a consequence of a larger torsional barrier (E_a) in the singlet excited state. An analysis of the vibrational structures observed in hexane and the correlations between fluorescence maxima and solvent polarity further suggested that the molecule becomes more planar in the excited state, and such a planar $^1t^*$ (ICT) state is responsible for the observed fluorescence in both nonpolar and polar solvents.[26] Values of k_f decrease with increasing solvent polarity, but the corresponding value of k_{nr} is slightly larger in acetonitrile vs hexane (Table 3). These changes account for the decrease in Φ_f with increasing solvent polarity.

The photochemical behavior of **1Me**, **1Cl**, and **1CF** is similar to that of **1H**: namely, other decay channels except for fluorescence and the double bond torsion are unimportant. It is interesting to note that both ED and EW substituents at the para position of the *N*-phenyl group enhance the fluorescence quantum yield (Table 3). Since the values of k_f are comparable for all four compounds in the same solvent, the origin of fluorescence enhancement could be attributed to an increase in the torsional barrier that decreases the rate of isomerization and thus the values of k_{nr} and Φ_{tc}. According to the 0−0 transition energies (Table 1), the $^1t^*$ state of **1H** is stabilized by ED substituents (e.g., **1Me**) but destabilized by EW substituents (e.g., **1CF**). To result in a larger torsional barrier for both cases, the $^1p^*$ state should be less stabilized in the former and more destabilized in the latter cases, as depicted in Figure 10. In other words, the substituent effect on the $^1p^*$ vs the $^1t^*$ state of **1H** should be different. This is indeed in accord with the model of resonance structures that was previously employed for the rationalization of the amino conjugation effect in *N*-phenyl- vs *N*-alkyl-substituted 4-aminostilbenes.[25] For the $^1t^*$ state, the amino lone pair electrons could delocalize to either the stilbene (resonance structure A) or the phenyl ring (resonance structure B) (eq 4). In principle, the importance of structure A would be enhanced by ED substituents but diminished by EW substituents, and the opposite would be true for structure B. Since structure A corresponds to the HOMO → LUMO transition, such a substituent effect agrees with the red vs blue shifts of the absorption spectra (Table 1) and the larger vs smaller values of μ_e for **1Me** and **1CF** vs **1H**, respectively. In contrast, the corresponding resonance structure A should be predominant in the $^1p^*$ state of **1H** (eq 5). As a result, a further enhancement of its contribution to $^1p^*$ by ED R substituents should be rather limited; however, a slight weakening of its contribution due to the presence of an EW substituent could significantly raise the energy of the $^1p^*$ state.

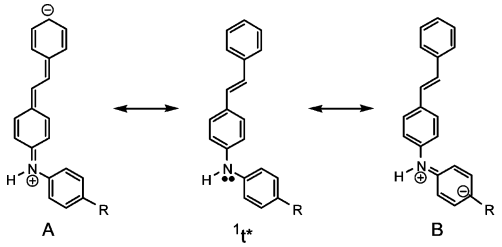

(4)

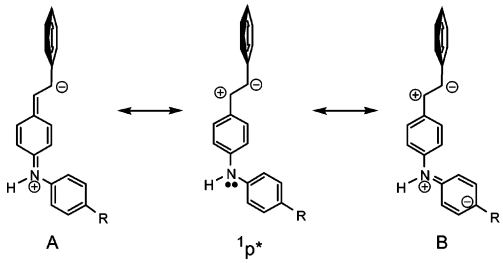

(5)

Excited-State Behavior of 1CN and 1CO (Group II). The phenomenon of dual fluorescence observed for **1CN** and **1CO** in dichloromethane and more polar solvents differentiates them from the other derivatives of **1**. The location of the long-wavelength emission band (λ_f = 517 nm in acetonitrile) and the corresponding value of μ_e (16.4 D) for **1CN** are reminiscent of the TICT fluorescence of DMABN (λ_f = 485 nm in acetonitrile and μ_e = 17 D).[6,13] Further, it has recently been reported that the TICT state of ethyl 4-(*N*-phenylamino)-benzoate, an analogue of **1CO**, dominates the fluorescence in polar solvents (e.g., λ_f = 486 nm in acetonitrile and μ_e = 17.7 D).[41] Indeed, as is demonstrated by the bridged model compound **3CN**, restriction of the rotation of the anilino-benzonitrilo C−N single bond removes the long-wavelength emission band and thus the dual fluorescence property. Moreover, **3CN** is strongly fluorescent in both polar and nonpolar solvents, in analogy to the behavior of the group I species. On the other hand, the long-wavelength emission band is retained and even enhanced for **4CN**−**6CN** (Figure 7), indicating that the rotation of the other single bonds plays a negligible role in accounting for the TICT state. Evidently, the formation of a DMABN-like TICT state is responsible for the low quantum yields of fluorescence for **1CN** in polar solvents. The weak emission property observed for the TICT state is consistent with the forbidden nature of the fluorescence. In addition, a broad TICT emission is in accord with the picture of a broad distribution of conformers with varied twisted angles around the C−N single bond. Since the photoisomerization quantum yield is also low for **1CN** in dichloromethane, the decay process of TICT → $^1p^*$ or $^3p^*$ should be unimportant, and the nonradiative decay of the TICT state might be mainly via internal conversion, as proposed for the other TICT systems.[20,42] The similarity in photochemical behavior between **1CO** and **1CN** also agrees with the common feature

(41) Ma, L.-H.; Chen, Z.-B.; Jiang, Y.-B. *Chem. Phys. Lett.* **2003**, *372*, 104−113.

of dual fluorescence in both methyl 4-(*N*,*N*-dimethylamino)-benzoate (DMABME) and DMABN.[8,10]

The presence of a TICT state in **1CN** also accounts for the temperature-dependent fluorescence spectra (Figure 5). For stilbenes such as the group I molecules that conform to the two-state mechanism (^{1}t* and ^{1}p*), the fluorescence intensity would be either decreased or nearly unchanged upon increasing the temperature, corresponding to the activated and unactivated processes of the double bond torsion in the singlet and the triplet excited state, respectively.[14] When there is an equilibrium TICT $\rightleftarrows$ ^{1}t*, the activated process TICT $\rightarrow$ ^{1}t* could compensate for the depopulation of ^{1}t* in the activated process ^{1}t* $\rightarrow$ ^{1}p* as long as the latter has a larger barrier (i.e., $E_a > E_a'$, Figure 9). In fact, the double bond torsion in **1CN** is more likely via the unactivated triplet mechanism, presumably due to a large E_a value (vide infra). As a result, the model of fluorescence kinetics previously derived for DMABN[7,13] could also apply to the case of **1CN**. Assuming that the change in fluorescence peak intensity is proportional to that in Φ_f, the values of both $\Phi_f(^1t^*)$ and Φ_f-(TICT) are increased but the ratio $\Phi_f(\text{TICT})/\Phi_f(^1t^*)$ is decreased upon increasing the temperature for **1CN** in acetonitrile (Figure 5). This is indeed consistent with an equilibrium between the two states in the temperature range of -40 to 50 °C (i.e., $k_d > k_f'$). A quantitative treatment of the spectra in Figure 5d was not performed due to the poorly resolved and incomplete fluorescence spectra.

Several pieces of evidence have suggested that the process of the C−N bond twisting toward the DMABN-like TICT state is negligible for **1CN** and **1CO** in the nonpolar solvent hexane: (a) The spectra show vibrational structures and no dual fluorescence. (b) The fluorescence quantum yields are high and the sum of $\Phi_f + 2\Phi_{tc}$ is close to unity. (c) The values of k_f are large and comparable to those of the group I compounds, in contrast to the low k_f values for the TICT fluorescence in polar solvents. (d) No fluorescence enhancement was observed for **1CN** in hexane upon heating from -40 to 50 °C. Instead, the fluorescence is only slightly perturbed, as previously observed for *trans*-*N*,*N*-diphenylaminostilbene (DPhAS),[25] indicating a triplet-state mechanism of photoisomerization. Since the cyano group is a strong EW group, the energy of the ^{1}p* state for **1CN** would be largely raised according to the substituent effect shown in Figure 10. On the other hand, the corresponding ^{1}t* state is not destabilized (Table 1), presumably due to the conjugation effect of the cyano group that compensates for its induction effect. As a result, the torsional barrier in the singlet excited state might be too high to be overcome at room temperature. This could account not only for the large value of Φ_f in hexane but also for the triplet-state mechanism of photoisomerization ($\Phi_{isc} = 2\Phi_{tc}$, $k_{isc} = \Phi_{isc}\tau_f^{-1}$). The non-radiative decay rate constant in hexane could thus be attributed to the rate constant for intersystem crossing (i.e., $k_{nr} \approx k_{isc} \approx 2.1 \times 10^8$ s^{-1}), a value nearly the same as that for DPhAS ($k_{isc} \approx 2.0 \times 10^8$ s^{-1}).[25] (e) The sigmodial curves in the plots of Φ_f against $E_T(30)$ (Figure 8) are analogous to the acid−base titration curves, which indicates that the "equivalent point" of the population of molecules in the TICT vs ^{1}t* state is not achieved until the solvent is more polar than THF.

Excited-State Behavior of 1OM (Group III). Despite the absence of well-resolved dual fluorescence in the steady-state spectra, the great similarity in the solvent- and temperature-dependent fluorescence behavior between **1OM** and the group II compounds indicates the presence of a TICT state for **1OM** in polar solvents. For example, the values of Φ_f for **1OM** also exhibit a sigmodial relationship with $E_T(30)$. In addition, the sum of $\Phi_f + 2\Phi_{tc}$ is also much less than 1.0 in dichloromethane but not in hexane. Furthermore, the fluorescence in acetonitrile is also enhanced upon heating. Therefore, the observed fluorescence could result from an overlap of the emission of the ^{1}t* and the TICT state, for two reasons: (1) the fluorescence band becomes much narrower when the TICT state formation is blocked (i.e., **4OM**, vide infra), and (2) the correlation of the fluorescence peak energies and the Hammett σ^+ constants predicts a less red-shifted maximum for the ^{1}t* fluorescence on going from hexane to dichloromethane and acetonitrile (Figure 4). Accordingly, the two states are both highly polar and the μ_e value reported in Table 2 for **1OM** should be considered as an average of their dipole moments. It should also be noted that, unlike the case of **1CN**, the photoisomerization of **1OM** is more likely involved with the singlet-state pathway, because the fluorescence decreases monotonically in hexane with increasing temperature (Figure 5a).

A comparison of the fluorescence behavior of **1OM**−**4OM** and **6OM** has offered a clue to the single bond that is responsible for the TICT state formation in **1OM**. A common feature observed for **1OM**−**3OM** and **6OM** is the dramatic decrease in Φ_f on going from hexane to acetonitrile (Table 3). In particular, the confinement of the central C═C bond in the fused ring does not prevent **6OM** from having a low value of Φ_f in acetonitrile. The solvent effect on Φ_f for **4OM** is different from those for the other methoxy derivatives but similar to that for the group I aminostilbenes, as is the case of **3CN** among **1CN**−**6CN**. Although a pure sample of **5OM** is not available, which precludes a direct examination of the role of the styrenyl-anilino C−C bond in the TICT state formation of **1OM**, the experience gained from the corresponding studies of **1CN**−**6CN** has allowed us to conclude that the TICT state of **1OM** is associated with the twisting of the stilbenyl-anilino C−N bond. Indeed, if the rotation of the styrenyl-anilino C−C bond played an important role in the excited-state behavior of **1OM**, it would affect **4OM** as well, but this is not the case. Such a unique TICT state formation observed for **1OM** could be attributed to the strong electron-donating methoxy substituent that results in a stronger amino donor than that in the other derivatives of **1**.

***N*-Alkyl- vs *N*-Aryl-Substituted Aminostilbenes.** The ICT states of several *N*,*N*-dimethylamino-substituted stilbenes, including the parent molecule DS,[15] the donor−acceptor-type 4-(*N*,*N*-dimethylamino)-4′-cyanostilbene (DCS)[16,17] and 4-(*N*,*N*-dimethylamino)-4′-nitrostilbene (DNS),[18] and the donor−donor-type 4,4′-tetramethyldiaminostilbene (DDS),[15,19] have been discussed by several research groups in favor of the TICT state formation in polar solvents, although their steady-state spectra lack dual fluorescence. In addition, despite the different nature of these aminostilbenes, all of their TICT states have been suggested to result from the twisting of the anilino-styrenyl C−C single bond and to be responsible for the observed fluorescence, even when the value of Φ_f is high for some cases. The emissive nature of the TICT state was then attributed to either a large

(42) (a) Maliakal, A.; Lem, G.; Turro, N. J.; Ravichandran, R.; Suhadolnik, J. C.; DeBellis, A. D.; Wood, M. G.; Lau, J. *J. Phys. Chem. A* **2002**, *106*, 7680−7689. (b) Nad, S.; Kumbhakar, M.; Pal, H. *J. Phys. Chem. A* **2003**, *107*, 4808−4816.

vibronic mixing with the other allowed states or an incomplete twisting of the single bond (i.e., twisted angle < 90°).

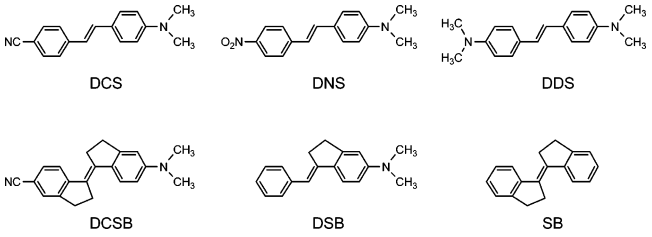

However, the arguments for such a three-state (^{1}t*, ^{1}p*, and TICT) model for these *N*,*N*-dimethylaminostilbenes have been challenged.[21−23] First, a large solvatofluorochromism does not necessarily correspond to a fluorescent TICT state, because the ^{1}t* state could be also highly polar, as shown by femtosecond dynamics for the case of DCS.[22,23] In addition, the implication of ^{1}t* → TICT based on the precursor−successor relationship observed in time-resolved fluorescence spectra could also be explained by the longitudinal dielectric relaxation of solvent molecules.[21,22] Further, the observation of lifetime maxima at intermediate temperature could be associated with the phase (e.g., melting or glass) transition of the solvent molecules instead of the presence of a fluorescent TICT state.[21] Moreover, the pronounced ring-bridging effect on the fluorescence quantum yield and the nonradiative decay rate for DCSB vs DCS and for DSB vs DS have been interpreted as results of the restriction of the C−C single bond rotation, in favor of the TICT model. However, the same phenomenon is also present for *trans*-1,1′-biindanylidene (SB) vs *trans*-stilbene, a system that conforms to the two-state (^{1}t* and ^{1}p*) model. Thus, the ring-bridging effect could be simply due to the methylene substituent effect that modifies the reaction hypersurface for the double bond torsion and/or induces new reactions.[32] Indeed, it has been shown that the torsional barrier for SB is intrinsically lower than that for *trans*-stilbene.[43]

A comparison of the fluorescence behavior between **1** and DS has led to a new challenge to the TICT model for DS.[44] On the basis of (1) the shape of the fluorescence spectra, (2) the relative values of $\Delta\nu_{1/2}$ and $\Delta\nu_{st}$, and (3) the response of Φ_f to the solvent polarity, the fluorescence behavior of DS is more like that of the group I rather than the groups II and III species of **1**. In particular, the excited-state dipole moment for DS is nearly the same as that for **1Me** and much lower than those for the TICT state of **1OM**, **1CN**, and **1CO**. The observations of (a) a much lower Φ_f value for **5CN** vs the other cyano derivatives in hexane and (b) a similar ratio of fluorescence quantum yields for Φ_f(**5CN**)/Φ_f(DSB) (28) and Φ_f(**1CN**)/ Φ_f-(DS) (25) in hexane also support a special methylene bridging effect that enhances the nonradiative decay. Despite such a special substituent effect, **5CN** still displays a large decrease in Φ_f on going from hexane to acetonitrile due to the C−N bond twisting. Therefore, it should be that either the TICT state proposed for DS is unimportant or the group I aminostilbenes possess a DS-like TICT state. However, regarding the distinct fluorescence properties observed for the group I vs groups II and III aminostilbenes, it would be difficult to understand why the consequence of the C−C bond twisting is so different from that of the C−N bond twisting in **1**.

Experimental Section

Methods. Electronic spectra were recorded at room temperature. UV spectra were measured on a Jasco V-530 double-beam spectrophotometer. Fluorescence spectra were recorded on a PTI QuantaMaster C-60 spectrofluorometer. The optical density of all solutions was about 0.1 at the wavelength of excitation. It should be noted that, unlike the uncorrected spectra previously reported in refs 25 and 26, the fluorescence spectra reported herein have been corrected for the response of the detector. The fluorescence spectra at other temperature were measured in an Oxford OptistatDN cryostat with an ITC502 temperature controller. A N_2-bubbled solution of anthracene ($\Phi_f = 0.27$ in hexane)[45] was used as a standard for the fluorescence quantum yield determinations of **1**−**6** in acetonitrile under N_2-bubbled conditions with solvent refractive index correction. An error of ±10% is estimated for the fluorescence quantum yields. Fluorescence decays were measured at room temperature by means of a PTI Timemaster apparatus with a gated hydrogen arc lamp using a scatter solution to profile the instrument response function. The goodness of nonlinear least-squares fit was judged by the reduced χ^2 value (<1.2 in all cases), the randomness of the residuals, and the autocorrelation function. Quantum yields of photoisomerization were measured on optically dense degassed solutions (~10^{-3} M) at 313 nm using a 75-W Xe arc lamp and monochromator. *trans*-Stilbene was used as a reference standard ($\Phi_{tc} = 0.50$ in hexane).[46] The extent of photoisomerization (<10%) was determined using HPLC analysis (Waters 600 controller and 996 photodiode array detector, Thermo APS-2 Hypersil, heptane and ethyl acetate mixed solvent). The reproducibility error was <10% of the average. MOPAC-AM1 and INDO/S-CIS-SCF (ZINDO) calculations were performed on a personal computer using the algorithms supplied with the package of Quantum CAChe Release 3.2, a product of Fujitsu Ltd. The X-ray diffraction measurements were performed on Bruker Smart-CCD diffractometers (λ = 0.71073 Å) at room temperature. Intensity data were collected in 1315 frames with increasing ω (0.3° per frame) and corrected for Lp and absorption effects using the SADABS program. The structures were solved by direct methods. Structural parameters were refined on the basis of F^2. All calculations were performed by using SHELXTL programs. All non-hydrogen atoms were refined anisotropically. Hydrogen atoms were assigned idealized locations and given isotropic thermal parameters 1.2× the thermal parameter of the carbon atoms (but 1.5× for the hydrogens in methyl groups) to which they were attached.

Materials. Solvents for organic synthesis were reagent grade or HPLC grade, but all were HPLC grade for spectra and quantum yield measurements. All other compounds were purchased from commercial sources and were used as received. The characterizations of compounds **1**−**6** are provided in the Supporting Information.

Concluding Remarks

The substituent-dependent excited-state behavior of the seven *N*-aryl-substituted 4-aminostilbene derivatives **1** has been elucidated and divided into three categories. The group I consists of **1H**, **1Me**, **1Cl**, and **1CF**, and their excited decay conforms to the two-state model. Aminostilbenes **1CN** and **1CO** belong to group II, the members of which display dual fluorescence in polar solvents. The short- and the long-wavelength emission bands have been attributed to the emission from the planar and

(43) (a) Saltiel, J.; D'Agostino, J. T. *J. Am. Chem. Soc.* **1972**, *94*, 6445−6456. (b) Rothenberger, G.; Negus, D. K.; Hochstrasser, R. M. *J. Chem. Phys.* **1983**, *79*, 5360−5367.

(44) In view of the inherent difference in electronic structures among donor-only, donor−acceptor-type, and donor−donor-type aminostilbenes, any comparison to be made between **1** and the *N*-alkyl derivatives should be more appropriately restricted to the same type of aminostilbenes, viz., the donor-only DS.

(45) Dawson, W. R.; Windsor, M. W. *J. Phys. Chem.* **1968**, *72*, 3251−3260.

(46) Malkin, S.; Fischer, E. *J. Phys. Chem.* **1964**, *68*, 1153−1163.

twisted ICT states, respectively. The group III compound is **1OM**, whose photochemical properties closely resemble the group II molecules and could also be described by the three-state model with an overlapped emission from the ^{1}t* and the TICT states. The TICT state formation in **1OM**, **1CN**, and **1CO** is only favorable in solvents more polar than THF. The corresponding studies on model compounds **2**−**6** have allowed us to deduce the TICT structures for the groups II and III compounds. Whereas the TICT state for **1CN** is DMABN-like, resulting from the twisting of the benzonitrilo-anilino C−N single bond, it is the stilbenyl-anilino C−N bond that twists in the case of **1OM**. Despite the difference in the bond that twists and in the direction of the ICT transition, the TICT states for **1OM** and **1CN** have the common features of broad fluorescence spectra and low fluorescence yields. These features are apparently different from the TICT states previously proposed for *N*,*N*-dialkylaminostilbenes such as DCS and DS. It is important to note that the basis of our TICT arguments relies on the close linkage of the steady-state fluorescence behavior for **1CN** and the TICT paradigm DMABN. A similar spectroscopic correlation between **1OM** and **1CN** in turn leads to the conclusion of the presence of a TICT state for **1OM**. In this case, the group I molecules have functioned as the "TICT-free controlled compounds", complementary to the bridged model molecules **3**−**6**. These important correlations would not be possible without the sensitive response of the fluorescence properties of **1** to the solvent polarity. In other words, the *N*-aryl amino conjugation effect is a sensitive probe for the "degree of conjugation" between the D and A groups of aminostilbenes in the excited states. By the same token, the similarity in solvent-dependent fluorescence properties for DS and the group I species suggests that there is no need to invoke a fluorescent TICT state for DS.[15] Further dynamic and theoretical studies on these and the related systems would complement the current results and provide more insights into the ICT states of aminostilbenes.

Acknowledgment. We thank the National Science Council of Taiwan, UST, and the NCU-ITRI Joint Research Center for financial support, Mr. Jyh-Wei Tu for the synthesis of compounds **3OM** and **3CN**, and Miss F.-L. Liao and Professor S.-L. Wang at the Instrumentation Center of National Tsing Hua University for resolving the crystal structures of **1CN**, **2CN**, and **1CO**.

Supporting Information Available: Detailed characterization data for aminostilbenes **1**−**6**; crystal refinement data for **1CN**, **1CO**, and **2CN**; solvatofluorochromic plots for **1**, **3CN**, and **4OM**; and fluorescence and excitation spectra of **1** in hexane and acetonitrile recorded by changing the excitation and emission wavelengths (PDF). X-ray experimental details (CIF). This material is available free of charge via the Internet at http://pubs.acs.org.

JA047604D